A STUDY OF METHODS USED IN

MEASUREMENT AND ANALYSIS OF SEDIMENT LOADS IN STREAMS

REPORT FF

MEASURING THE SURFACE AREA OF SEDIMENT PARTICLES

1984

A Study of Methods Used in

MEASUREMENT AND ANALYSIS OF SEDIMENT LOADS IN STREAMS

A Cooperative Project

Sponsored by the

Interagency Advisory Committee on Water Data

Subcommittee on Sedimentation

Participating Agencies

Agricultural Research Service
Corps of Engineers ** Geological Survey
Forest Service ** Bureau of Reclamation
Federal Highway Administration ** Bureau of Land Management

REPORT FF

MEASURING THE SURFACE AREA OF SEDIMENT PARTICLES

By

John V. Skinner

Prepared for Publication by the Staff of the
Federal Inter-Agency Sedimentation Project
St. Anthony Falls Hydraulic Laboratory
Minneapolis, Minnesota

Published by
U.S. Army Engineer District, St. Paul

1984

CONTENTS

ILLUSTRATIONS

TABLES

MEASURING THE SURFACE AREA OF SEDIMENT PARTICLES

By

John V. Skinner

ABSTRACT

Light traveling through a suspension of water and fluvial sediment is scattered and absorbed by the particles. Several investigators have studied this attenuation process in an effort to devise optical techniques for measuring sediment concentration. Unfortunately, most of these efforts have not been successful because the relationship between attenuation and concentration is strongly influenced by the size distribution of the sediment particles. In this report, an analysis of experimental data shows that the attenuation of infrared light is closely correlated with the total geometric surface area (GSA) of the particles suspended in a unit volume of the water. The GSA of an individual particle is defined as the area of a sphere having a diameter equal to the particle's diameter. The correlation between attenuation and total GSA holds for a broad range of particle diameters. The lower limit is about 2 μm; the upper limit is greater than 115 μm, the diameter of the largest particles tested. The range in GSA per unit volume extends from zero to more than 0.055 square meters per liter. The latter value is equivalent to full-

scale deflection on the infrared light meter.

INTRODUCTION

The interaction between light and sediment particles has attracted the interest of many hydrologists and oceanographers involved in sediment-transport studies. This interest originates from a need for an accurate, inexpensive instrument that continuously registers the concentration of sediment particles suspended in surface waters.

Investigators have attempted to estimate sediment concentration by following a two-step procedure. First, they measure the intensity of a collimated light beam where it emerges from a mixture of water and sediment. Then they use a calibration chart to convert the intensity reading to a concentration value. The rationale behind this procedure is based on qualitative information obtained from visual observations and on quantitative data obtained from certain experiments. If a transparent container full of clear water is illuminated with a collimated beam, most of the light passes directly through the water. If a small quantity of sediment is now mixed with the water, the sediment particles scatter and absorb some of the light and thereby lower the intensity of the emergent beam. Data for a calibration chart can be collected by repeatedly adding measured quantities of sediment and then, after each addition, recording the intensity of the beam. A plot of these data forms a monotonic function that, by definition, relates any single intensity reading to only one value of concentration. If the entire calibration procedure is repeated many times, all of the monotonic

functions will be identical only if all the sediment specimens have the same physical and optical properties. These properties include such things as refractive index, color, density, and particle-size distribution.

When used outside the laboratory in more pragmatic situations, this concentration-measurement procedure has an operational record dotted with successes and failures. Manufacturers of certain powders, such as cement and paint pigment, have reported many successful applications. Specimens of these powders have a high degree of uniformity that probably stems from the carefully controlled manufacturing processes. These successful applications have led to the development of the turbidimeter--a special optical instrument for measuring concentration. Some turbimeters have pre-calibrated meters that register directly in concentration units; however, tests indicate that caution must be exercised in interpreting the readings. In contrast with manufacturers, researchers in the fields of hydrology and sedimentology have generally failed in attempts to use the concentration measurement technique. For river-born sediments, the relationship between emergent-light intensity and sediment-concentration is influenced by the geographic source of the sediment. In general, samples taken from different rivers have different intensity-concentration relationships; furthermore, for any given river the relationship is likely to be unstable in the sense that it shifts with the passage of time and with variations in river stage.

The source of the problem in correlating light-intensity readings with fluvial-sediment concentration is revealed by some classical laws of optics. These laws indicate the intensity readings are more closely

related to the total surface area of the sediment particles than to the mass concentration of the particles. This surface-area relationship is not only interesting from the academic standpoint but it may also have some value in studying the adsorptive properties of fluvial sediments and their capacity to transfer water-born pollutants.

Purpose and Scope

This report describes the results of an investigation to examine the relationship between emergent light intensity, sediment concentration, and sediment surface area. The first portion of this study is based on experimental data collected by Szalona (1984, figure 2 and table 1) who tested an optical instrument that was unusual because it transmitted light in the infrared range of the electromagnetic spectrum. The more commonly used instruments transmit light in the visible range of the spectrum. The second portion of this study is based on some universal optical relationships that are examined in an effort to guide future development work.

REVIEW OF BASIC THEORY

An instrument that responds to light transmitted through a water-sediment suspension is governed by two relationships. The first relationship, the Lambert-Beer Law, is universal in that it applies to any suspension of particles dispersed in fluid. The second relationship, termed the circuit-parameter function, is restrictive in that it is set by electronic characteristics of the particular instrument used to sense the emergent beam. The two relationships are represented in block diagram form on figure 1. On this diagram, I_o and I are, respectively, (a) the intensity of the beam that enters a water-sediment suspension, and (b) the intensity of the beam that emerges from the suspension and strikes a photodetector. R is the reading on a meter connected to a circuit that amplifies the photodector's electrical output.

The Lambert-Beer Law, associated with the upper block on figure 1, is

$$I=I_o e^{\mu} \qquad (1)$$

where $\mu=-n\,\pi\,d^2K\ell/4$

In the preceeding equation,

d = the diameter of the particles suspended in the light beam;

n = the number of particles suspended in the light beam;

ℓ = the optical path-length within the water-sediment mixture; and

K = an optical scattering coefficient that depends upon the diameter of the particles, the refractive index of the particles, the wave-length of the light, and the refractive index of the water.

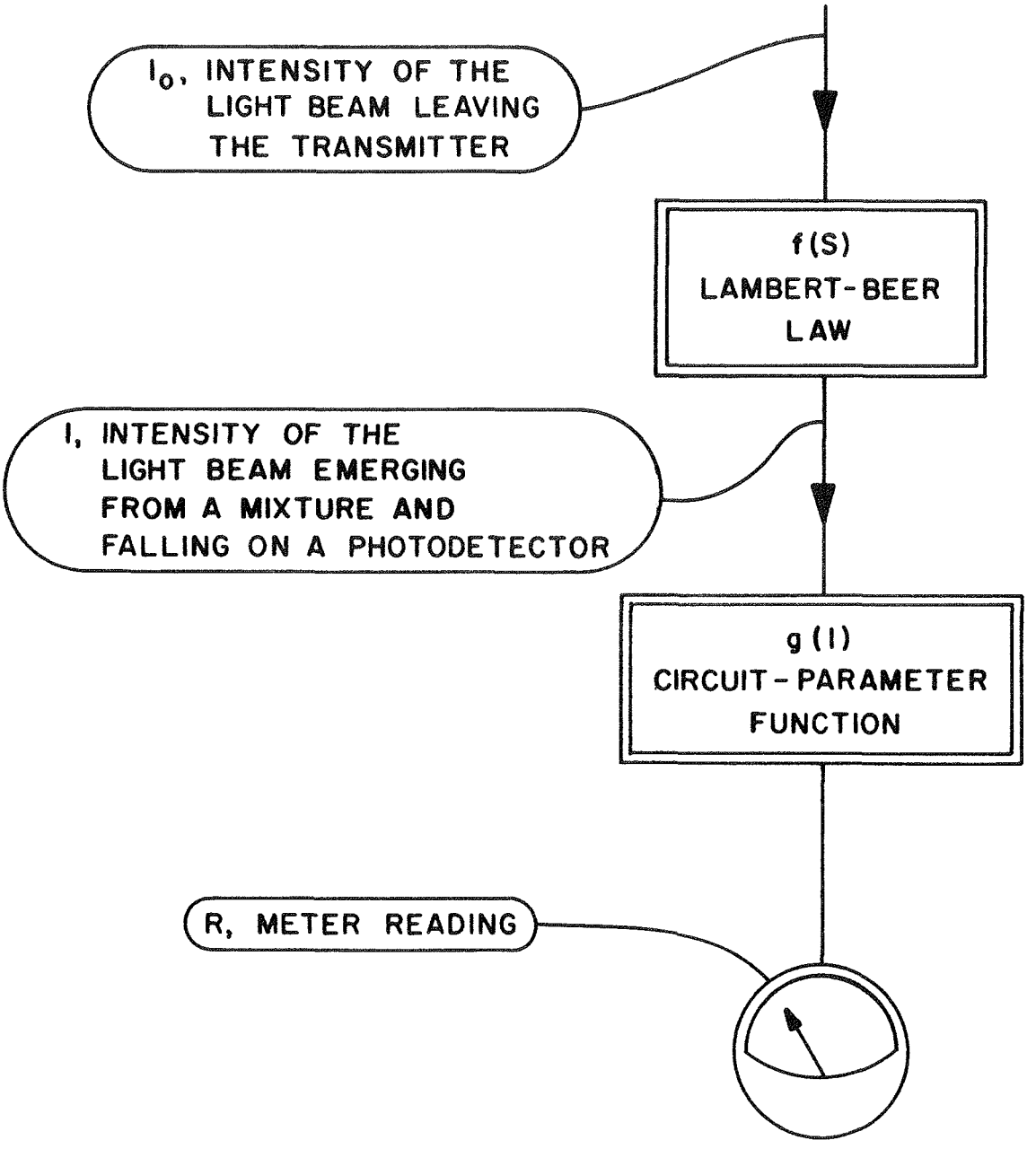

Figure 1.--Diagram of optical and electrical relationships that govern transmission-type instruments.

Combining the preceeding equation with g(I), the circuit-parameter function associated with the lower block on figure 1, we obtain the following:

$$R=g(I_o e^{\mu}) \qquad (2)$$

The preceeding expression shows that surface area plays a major role in determining the value of R. Notice that the exponent in the expression contains the product $(n \pi d^2)$ which equals the total surface area of "n" spherical particles each having a diameter "d". When equation 2 is applied to a specific instrument we can evaluate the "g" function experimentally; alternatively, we can bypass this step and deal with another equation of the form R = h(A) where "A" designates surface area. The function "h", which can also be evaluated experimentally, is simply the calibration curve that relates meter readings to surface areas.

Up to this point, the basic approach to measuring surface-area appears to be straightforward; however, when we apply the method to river sediments, some uncertainties and complications develop. For example, equation 1 applies to a suspension that has rather unusual properties: all the particles are spheres and all have the same diameter. In contrast, a suspension of river sediment fails to meet either of these requirements. Particles of river sediment have rough, irregular shapes and span a wide range of sizes. As an example of another difficulty, consider the problem of assigning a value to the factor K in equation 1. If all particles in a suspension have the same refractive index, the

assignment is straightforward; unfortunately, river-born particles have widely different indices of refraction. Some particles do not absorb light and therefore have a K value that is real. The remaining particles absorb some light and, according to optical theory, have a K value that consists of a real component and an imaginary component.

Although some difficulties exist in applying the Lambert-Beer Law to fluvial sediments, it is reasonable to expect that surface area will have a strong influence on light readings. In this paper, we gage the extent of this influence by examining Szalona's (1984) experimental data.

DESCRIPTION OF THE TEST APPARATUS

A cross-sectional view of the experimental apparatus is shown on figure 2. The light-emitting diode (LED) transmits a beam of infrared light into the sediment-water mixture which is shielded from stray outside light by the opaque-plastic cover. The walls of the container, which are also opaque, hold a sliding seal that aligns the photodetector with the LED. The tube that passes through the seal can be shifted to adjust the optical path length, labeled "gap" on the drawing. Circuits in an instrument box (not shown) alternately turn the LED on and off at a frequency of about 50 hz; other circuits supply a meter with an amplified photodetector signal. The reading on this meter is related to the intensity of the light that strikes the photodetector, however, the meter responds in an unusual fashion. If the light shifts to a lower intensity,

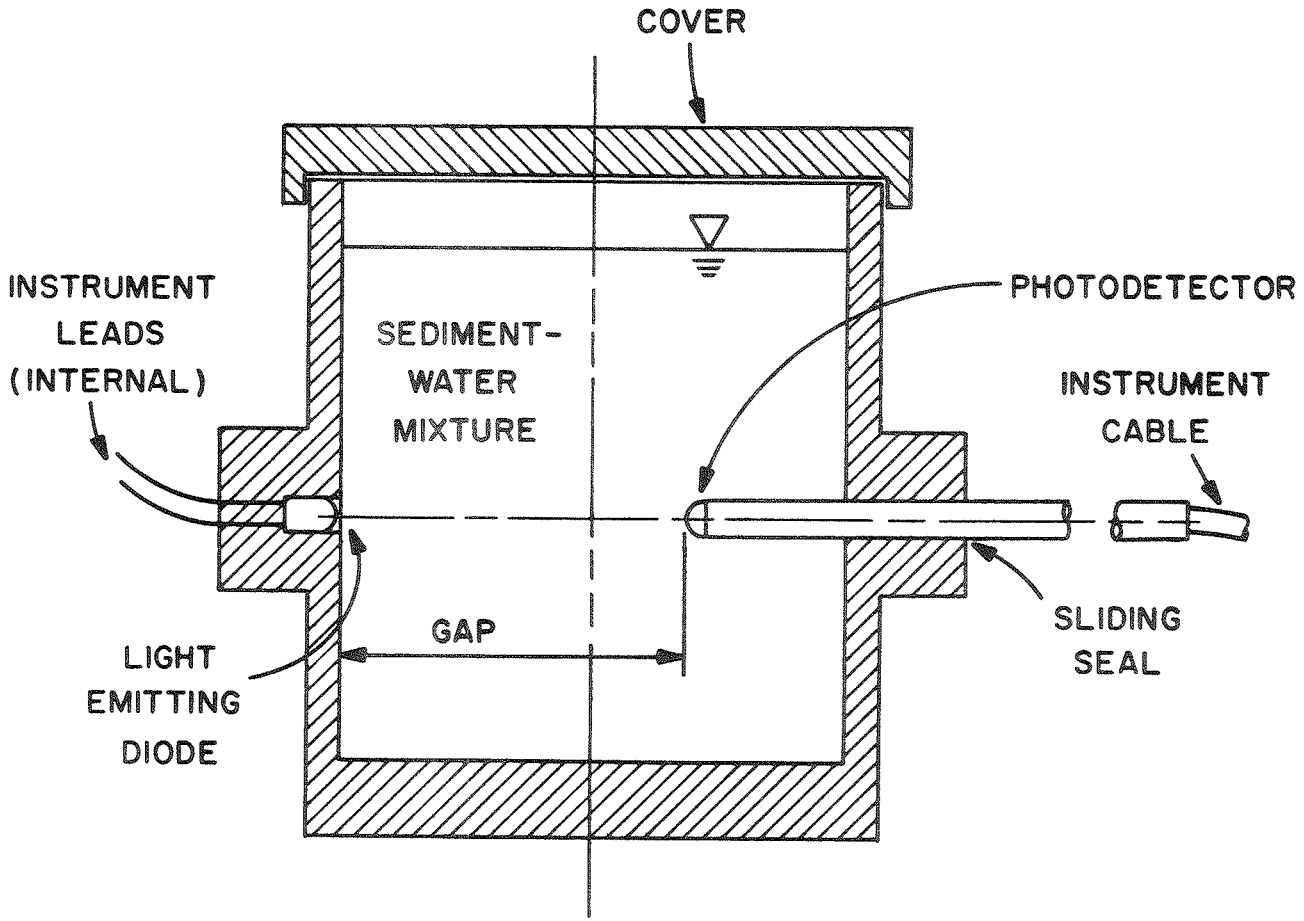

Figure 2.--Cross-sectional view of the test instrument (Szalona, 1984).

the meter shifts to a higher reading. The instrument box and the apparatus shown on figure 2 were made by Markland Specialty Engineering, Etobicoke, Ontario, Canada.*

QUALITATIVE ANALYSIS OF DATA

Before numerically analyzing the experimental data, let us explore some properties revealed by the general trends of the plotted lines on figure 3. The fan-shaped pattern of the plot emphasizes the problem in establishing a single calibration curve that applies to all sediment mixtures. Notice that the slopes of the calibration lines are sensitive to the size of the particles in suspension. Shifts in particle-size produce serious errors in measured concentration unless the instrument is promptly recalibrated. In some rivers, the size of suspended particles will shift frequently, so the recalibration task ranges from burdensome to impossible.

* Trade names are included for identification purposes only and do not constitute endorsement by the United States Government.

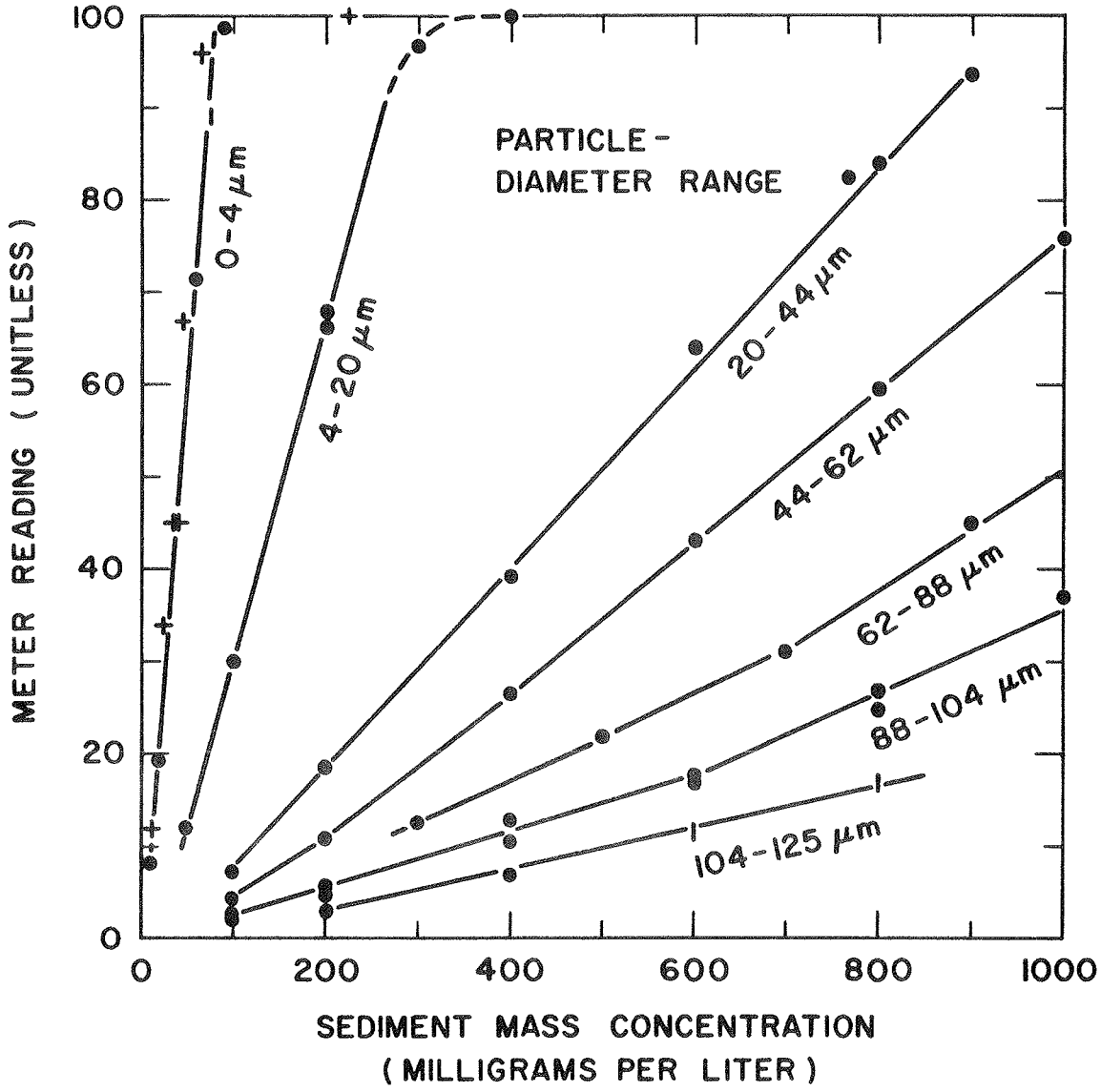

Figure 3.--The instrument's response to several particle-size fractions of sediment from West Bitter Creek, Okla. The short vertical lines represent a range of readings where single values could not be determined. The +'s represent datum points for the 1.4- to 4-µm group. The gap was set at 90 mm (Szalona, 1984).

On figure 3, the trend between line slope and particle size reinforces the hypothesis that surface area plays a key role. After selecting any two lines on figure 3, we see that for a given concentration the "small particle" line is associated with the greater of two meter readings. Because a high reading indicates a low light intensity, the suspension containing the small particles absorbs more light. The relation between particle size, surface area, and concentration may not be immediately obvious. Let us select a point on one of the lines and then move vertically upward to a point on the adjacent line. These two points represent mixtures having equal mass concentrations; however, the upper point represents a mixture with a greater surface area. The fact that surface area increases as particle size decreases can be visualized from a conceptual experiment. If we cut through a particle to create two smaller particles, additional surface becomes exposed at the cut. If both of the fragments are cut, more surface area is exposed. If the cutting process is continued, four trends develop: the number of particles increases, the surface area increases, the size of the particles decrease, and the total mass of the particles remains unchanged.

A discussion of surface area is facilitated by coining the term "surface-area concentration". We will define this term as the total surface area of all particles in a mixture divided by the volume of the mixture. The term is analogous to "mass concentration" defined as the total mass of all particles in a mixture divided by the volume of the mixture.

ASSUMPTIONS AND BASIC AREA EQUATIONS

A quantitative analysis of Szalona's (ibid, 1984) data is based on the following three assumptions that pertain to his test particles taken from West Bitter Creek in Oklahoma:

(a) all of the particles were spherical in shape.

(b) all of the particles had a density of 2650 kg/m^3, the density of quartz.

(c) all of the particles within a size-class interval were the same size. This size corresponded to the midpoint of the interval. For example, figure 3 indicates one group of particles in the size-class interval from 4-20 micrometers (μm). In the following analysis, these particles will be assigned a diameter of 12 μm, the arithmetic mean of the size-class boundaries.

An equation relating surface area, mass concentration and particle diameter can now be derived from the three assumptions. Consider a mixture having a volume of "Q"-liters and containing "n" particles all with a diameter of "d" μm.

The surface-area concentration of the mixture is

$$A_G = [n\pi d^2/Q] \times 10^{-12} \qquad (3)$$

where A_g is expressed in square meters per liter (M^2/L).

The mass concentration, C, of the mixture is proportional to $nV\rho$ where V is the volume of a single particle and ρ is its density (2650 kg/m^3). After deriving a proportionality constant to account for the desired

units, we can write

$$C = (0.442 \times 10^{-9})(n\pi d^3/Q) \qquad (4)$$

where C is expressed in milligrams per liter (mg/L).

After substituting equation 4 into equation 3, we obtain

$$A_g = 2.26 \times 10^{-3} (C/d) \qquad (5)$$

Equation 5, which will be used repeatedly in the following sections, shows that for a given mass concentration the surface-area concentration is inversely proportional to particle diameter.

MONODISPERSE MIXTURES

This section pertains exclusively to the data plotted on figure 3. Hypothetically, each meter reading on the graph is closely correlated with the surface area of the particles in suspension. To test this hypothesis, a few data points will be used to establish a regression equation that relates surface areas, A, to meter readings, R. This regression equation will establish the functional relationship R = h(A) that in turn will be applied to the remaining data on the graph. Let A_g designate the area computed from equation 5, and let A_ℓ designate the area computed from the regression equation. If the area hypothesis is correct, all data on figure 3 should reduce to a group of points that plot along a single line in an A_g - A_ℓ coordinate system.

Coefficients for the regression equation can be computed from data for any line on figure 3. Since the line marked "62-88 μm" lies near the center of the radial pattern, data for this line will be used. On

table 1, the first and second columns show C and R respectively, both being experimental data from figure 3. The third column shows the particle diameter, 75 μm, the midpoint of the 62-88 μm class interval. The fourth column shows A_g computed from equation 5.

Table 1.--Data for computing the regression equation

C, concentration in mg/L	R, meter reading	d, particle diameter in μm	A_g, surface area concentration in M^2/L
300	12.5	75	0.0090
500	22.0	75	0.0151
700	31.0	75	0.0211
900	45.0	75	0.0271

Taking the least-squares linear regression of A_g on R we obtain the desired regression,

$$A_\ell = 0.00266 + 0.000558\ R \qquad (6)$$

At this stage, it may be helpful to reexamine the significance of A_ℓ in equation 6. Ideally, a discussion of surface area must be supported by data on the area's "true" value. Because true-value data are not available, we must compute approximate values, based on an assumed shape or "geometry" of the particles. Interpreting A_g as a quasi-true value, we now compare it to A_ℓ, an area computed from a light-meter reading denoted R. To develop the regression equation that relates A_ℓ and R, we use A_g values; however, to prevent the area comparison from becoming completely circuitous, we use only a small portion of the A_g dataset.

Having established the regression formula (equation 6), we now apply it to all the data on figure 3. Results of the computations are shown in table 2. The first column shows particle-diameters followed in parenthesis by size-class intervals. The second and third columns show, respectively, the measured values for R, and the measured values for C. The fourth column shows A_g values computed from equation 5. The fifth column shows A_ℓ values computed from equation 6. Figure 4 graphically compares the A_g and A_ℓ values listed in table 2.

Figure 4 plot indicates a high degree of correlation ($r = 0.99$) between A_g and A_ℓ ; however, the plot does not include data for the 0.7 μm particles. These data, which are listed on the first four lines of table 2, fail to follow the established trend. In a later section, we examine some possible reasons for this disparity.

POLYDISPERSE MIXTURES

In this section, we again test the area hypothesis by applying the area equations to polydisperse mixtures that contain two, three, or four different particle sizes. The value of A_g for a polydisperse mixture that contains "k" sizes of particles is the sum of "k" surface areas. Stated in equation form,

$$A_g = 2.26 \times 10^{-3} \sum_{i=+1}^{k} C_i/d_i \qquad (7)$$

Data for 17 polydisperse mixtures are listed in table 3. Column 1 shows sample numbers assigned for identification purposes. Columns 2, 3, 4, and 5 show the concentration of the particles in the four particle-size intervals indicated across the top row of the table. Column 6 shows meter readings, R, obtained in the experiment (ibid, Szalona, table 1).

Table 2.--A_g and A_ℓ values for monodisperse mixtures.

d, particle diameter in μm	R, meter reading	C, concentration in mg/L	A_g, surface area concentration in M^2/L	A_ℓ, surface area concentration in M^2/L
0.7	8.0	10	0.0323	0.0071
(0 - 1.4)	19.5	20	0.0646	0.0135
	72.0	60	0.1940	0.0428
	98.5	90	0.2910	0.0576
2.7	12.0	12	0.0100	0.0094
(1.4 - 4)	34.0	25	0.0209	0.0216
	45.0	40	0.0335	0.0278
	67.0	45	0.0377	0.0400
	96.0	70	0.0586	0.0562
12	12.0	50	0.0094	0.0094
(4 - 20)	30.0	100	0.0188	0.0194
	66.0	200	0.0377	0.0395
	68.0	200	0.0377	0.0406
	97.0	300	0.0565	0.0568
32	7.5	100	0.0071	0.0069
(20 - 44)	18.5	200	0.0141	0.0130
	39.0	400	0.0283	0.0244
	64.0	600	0.0424	0.0384
	82.5	770	0.0544	0.0487
	84.0	800	0.0565	0.0495
	94.0	900	0.0636	0.0551
53	4.5	100	0.0043	0.0052
(44 - 62)	11.0	200	0.0085	0.0088
	26.5	400	0.0171	0.0174
	43.0	600	0.0256	0.0267
	59.5	800	0.0341	0.0359
	76.0	1000	0.0426	0.0451
75	12.5	300	0.0090	0.0096
(62 - 88)	22.0	500	0.0151	0.0149
	31.0	700	0.0211	0.0200
	45.0	900	0.0271	0.0278
96	3.0	100	0.0024	0.0043
(88 - 104)	2.0	100	0.0024	0.0038
	6.0	200	0.0047	0.0060
	4.5	200	0.0047	0.0052
	13.0	400	0.0094	0.0099
	10.5	400	0.0094	0.0085
	18.0	600	0.0141	0.0127
	17.0	600	0.0141	0.0121
	27.0	800	0.0188	0.0177
115	3.0	200	0.0040	0.0043
(104 - 125)	7.0	400	0.0079	0.0066
	11.5	600	0.0118	0.0091
	17.0	800	0.0158	0.0121

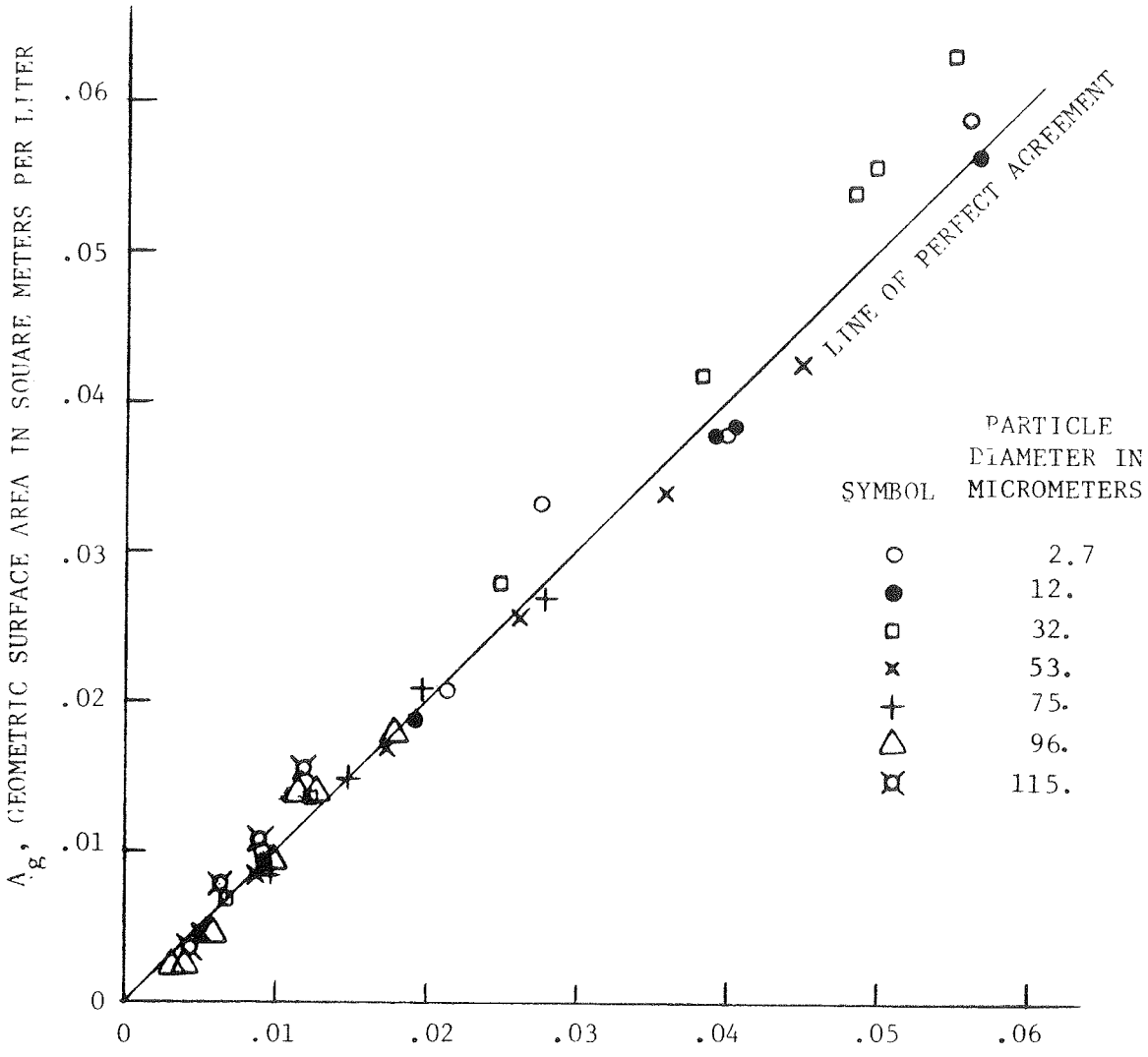

Figure 4.--Comparison of A_g and A_ℓ for monodisperse mixtures.

Column 7 shows A_g values computed from equation 7 and column 8 shows A_ℓ values computed from equation 6.

Figure 5, a plot of values listed in table 3, indicates a high degree of correlation ($r = 0.99$) between A_g and A_ℓ. For each mixture the instrument registers the total surface-area concentration of all size fractions present.

THE SCATTERING COEFFICIENT

In deriving equations for A_g and A_ℓ, we tacitly assumed that K, the scattering coefficient in equation 1, was independent of particle diameter. In this section, we examine the validity of this assumption. The scattering coefficient is equal to a particle's light-scattering cross-sectional area divided by the particle's geometric cross-sectional area; the latter value being $\pi d^2/4$ for a sphere. It may seem that these two cross-sectional areas should be equal; however, Orr (1959, p. 104-105) indicates that equality is more the exception than the rule. Oster (1948, p. 332) shows that K varies with particle size and ranges from zero to a maximum of from 3 to 5.

Sinclair (1950, p. 94), who worked primarily with aerosols, developed a plot known as the "Universal Scattering Curve." Orr and DallaValle (1959, p. 119) presented a slightly modified version of this plot which is reproduced on figure 6. As figure 6 shows, K is a function of the dimensionless variable X given by:

$$X = (d/\lambda)[(m^2-1)/(m^2+2)] \qquad (8)$$

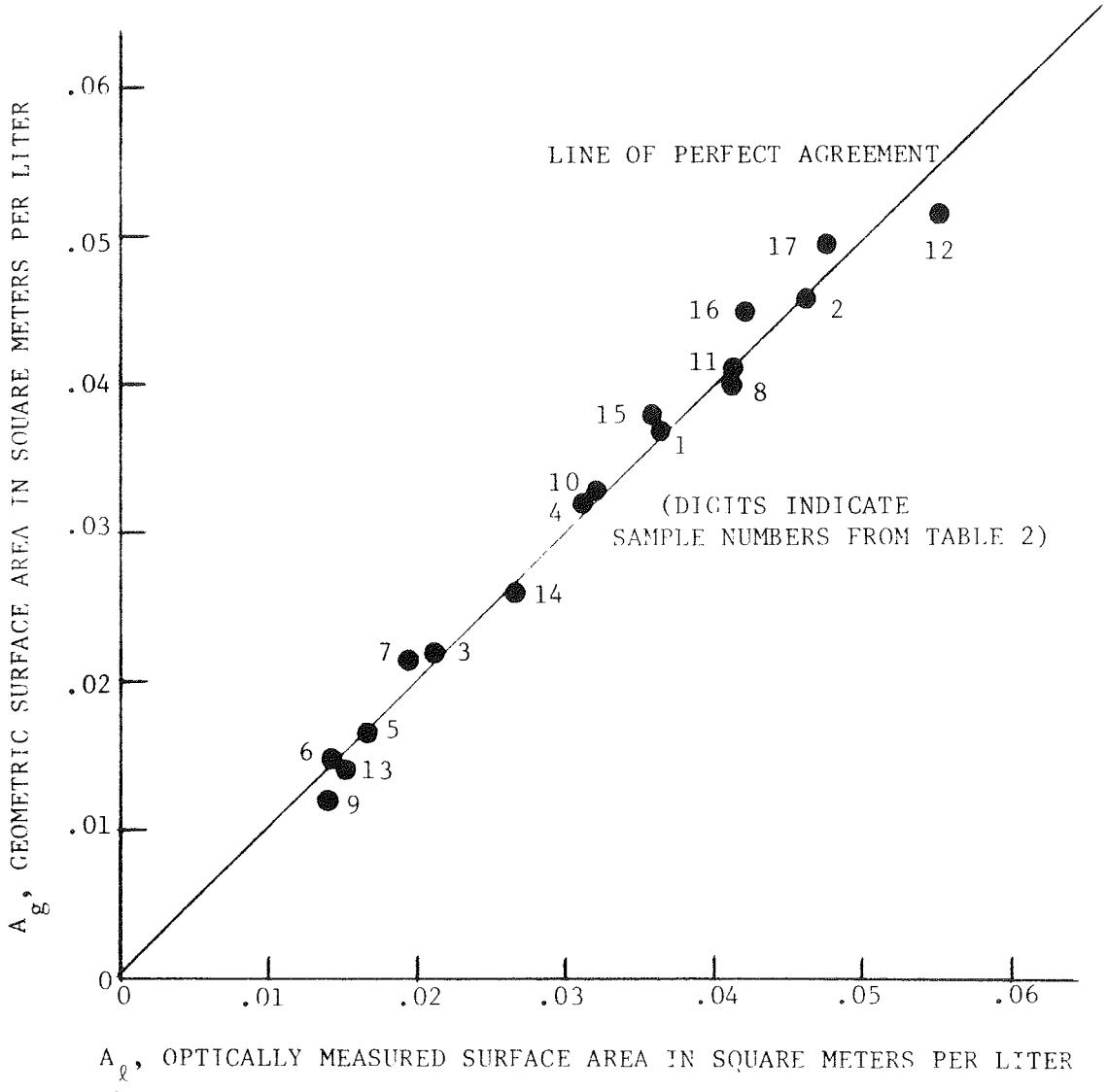

Figure 5.--Comparison of A_g with A_ℓ for polydisperse mixtures.

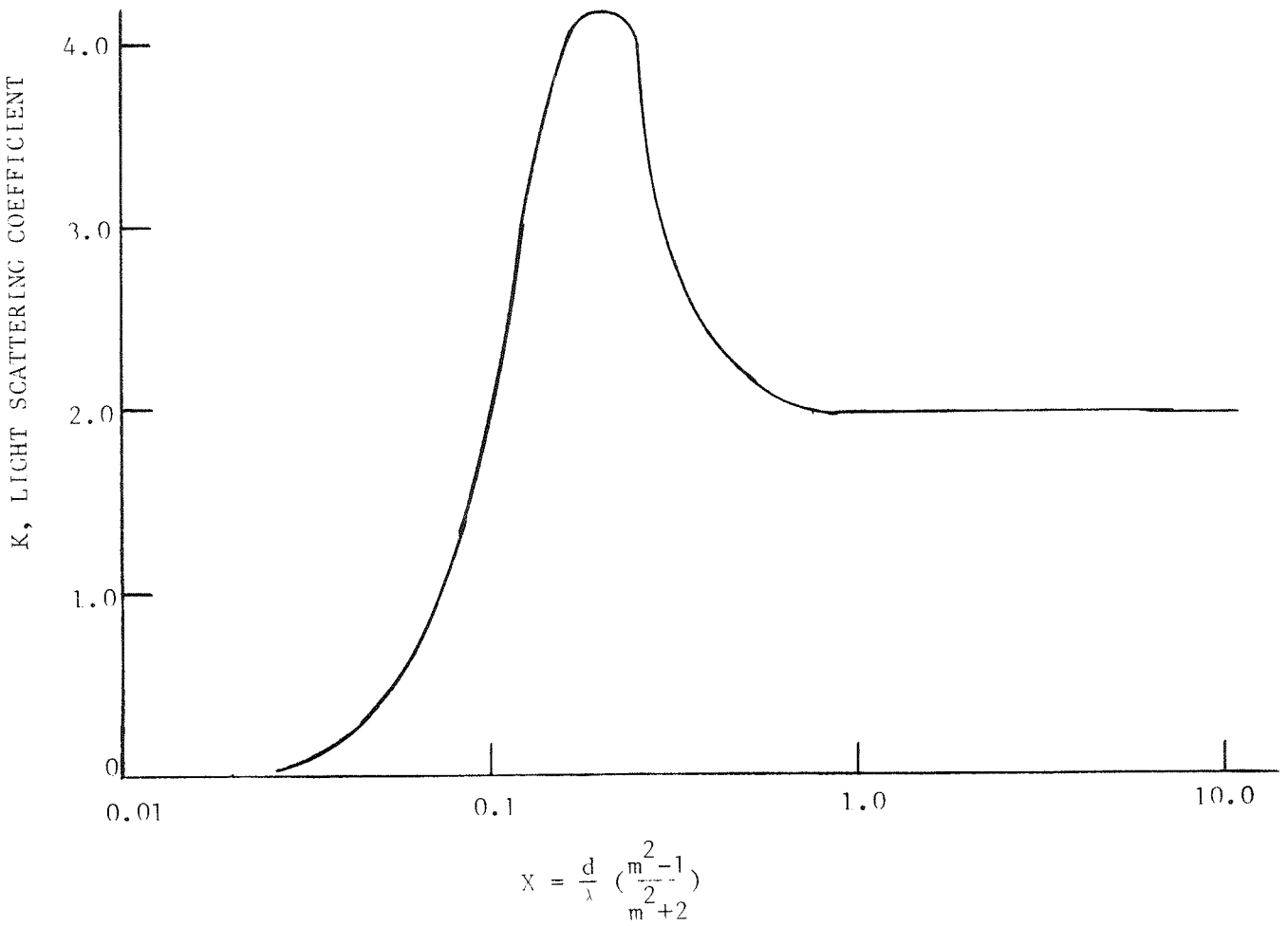

Figure 6.--Sinclair's Universal Scattering Curve.
After Orr and DallaValle, 1959, "Fine Particle Measurement," The Macmillan Company, New York.

In this equation:

d = diameter of the particles suspended in a fluid

λ = wavelength of the light impinging on the particles, and

m = the refractive index of the particles divided by the refractive index of the fluid (in our case, water)

Because the K values on figure 6 are real (as opposed to values that are complex), the curve applies only to nonabsorbing particles. Furthermore, because the curve is an approximation, the indicated K values may differ considerably from experimentally measured values.

The Universal Scattering Curve indicates that K equals 2.0 if X exceeds a critical value of about 0.6. This critical value is related to a critical particle diameter, d_c. For quartz particles suspended in water, table 4 shows critical particle diameters for two wavelengths: 0.2 μm (radiation in the ultra-violet range) and 0.90 μm (radiation used in Szalona's tests). Most of the data in table 2 and all of the data in table 3 pertain to particles larger than 9.1 μm; consequently, it is not surprising that the area computations compare favorably when K is assumed to be independent of particle diameter. What is surprising is the fact that data for the 2.7 μm particles, which are subcritical in size, (see table 2 and figure 4) agrees closely with data for the larger particles, which are supercritical in size.

The discrepancy between A_g and A_ℓ for the 0.7 μm particles can be explained with the aid of figure 6. Using refractive index values for quartz and water, we obtain 0.046 and 0.4 respectively for X and K. Let

Table 3.--A_g and A_ℓ values for polydisperse mixtures.

Sample number	Particle-size interval, in μm: 4-20 (d, particle diameter, in μm: 12)	20-44 (32)	44-62 (53)	62-88 (75)	R, meter reading	A_g, surface area concentration in M^2/L	A_ℓ, surface area concentration in M^2/L
	C, mass concentration in mg/L						
1	0	200	400	200	60.0	0.0375	0.0361
2	50	200	400	200	78.0	0.0469	0.0462
3	0	200	200	0	34.0	0.0226	0.0216
4	50	200	200	0	51.0	0.0321	0.0311
5	50	100	0	0	25.0	0.0165	0.0166
6	0	0	200	200	20.5	0.0145	0.0141
7	0	100	200	200	30.0	0.0216	0.0194
8	100	100	200	200	69.5	0.0405	0.0414
9	50	50	0	0	21.0	0.0130	0.0144
10	100	200	0	0	53.0	0.0330	0.0323
11	100	200	200	0	70.0	0.0415	0.0417
12	200	200	0	0	94.0	0.0518	0.0551
13	56	56	0	0	23.0	0.0146	0.0155
14	100	100	0	0	43.0	0.0260	0.0266
15	150	150	0	0	59.5	0.0389	0.0359
16	150	150	150	0	70.0	0.0453	0.0417
17	150	150	150	150	80.0	0.0498	0.0473

us now compare this K value with 2.0, the value for supercritical particles. The quotient of these two K values (0.4/2) indicates the theoretical value for the quotient A_ℓ/A_g for the 0.7 μm particles is 0.2. This theoretical value compares favorably with 0.21 obtained by averaging four A_ℓ/A_g quotients computed from data on the first four lines of table 2.

Data from the Universal Scattering Curve agrees closely with experimental data for the 0.7 μm particles. However, data from the Universal Curve differs considerably from experimental data for the 2.7 μm particles. The exact cause of this discrepancy is unknown: it may be related to experimental difficulties that Szalona (ibid, 1984) encountered in separating particles within the two smallest size fractions. The small size of the LED is another possible cause of the discrepancy. Ideally, the light source should have a large diameter and should transmit a beam of uniform intensity. The close proximity between the particles and the photodetector may be another cause of the discrepancy. Ideally, the distance between the particles and the detector should be several meters. Sinclair (1950, p. 90) found that the distance from the particles to the photodetector must be greater than 5.5 meters in order to obtain a K value of 2.0 for large particles.

Significant differences exist between an ideal system and the IR instrument on figure 2. Additional tests will be required to accurately chart the IR system's response to particles smaller than about 2 μm in diameter.

CONCLUSIONS AND SUGGESTIONS FOR FUTURE INSTRUMENT DEVELOPMENT

Test data for monodisperse and polydisperse mixtures of riverborn particles indicate that the infrared turbidimeter may be calibrated to register geometric surface-area concentration if the particles are larger than about 2 μm in diameter and smaller than about 115 μm. This second value was set by limits in the data-collection program: particles larger than 115 μm were not tested.

With additional development work, it may be possible to enhance the IR instrument's characteristics and to adapt the instrument for field use. The following paragraphs outline three topics that warrant particular attention.

The first topic pertains to extending the instrument's range in particle size. Sinclair's Universal Scattering Curve indicates the instrument's upper limit on particle size is probably greater than 115 μm. Additional tests should be performed to chart the instrument's response through the size range from 115 μm to 250 μm. Particles with diameters larger than 250 μm are rarely found in suspended-sediment samples. If the particles are present, they usually account for only a small fraction of the total surface area represented by all of the particles in the sample. A problem of more significant proportions is the instrument's lower limit on particle size. Sinclair's (1950) Universal Scattering Curve and Szalona's (1984) experimental data both indicate that the relationship between surface-area concentration and instrument readings is very complicated for particles smaller than about 2 μm. In many

samples, a significant proportion of the particles are in the clay-size range. Table 4 shows that it may be possible to decrease the lower size limit by using light with a wavelength shorter than infrared. The last line in this table indicates that the critical particle diameter drops from 9.1 μm down to 1.2 μm if the wavelength is shifted from 0.9 μm down to 0.2 μm. The 0.2 μm wavelength lies in the ultraviolet range, and can be generated and detected by small devices that are commercially available. Because the Universal Scattering Curve is an approximation, this expected shift in critical diameter must be confirmed by laboratory tests.

Table 4.--Critical particle diameters for two wavelengths.

Light wavelength, λ, in μm	0.2 (Ultra-violet)	0.9 (Infrared)
Refractive index of quartz	1.56	1.45
Refractive index of water	1.35	1.33
m, relative refractive index of quartz in water	1.16	1.09
$(1/\lambda)\ [(m^2-1)/(m^2+2)]$	0.52	0.066
d_c, critical diameter in μm for X = 0.6	1.2	9.1

The second topic pertains to improving the surface-area calibration procedure. If a fissure extends from the surface of a particle down into the interior, the walls of the fissure can become an active chemical adsorber. If the particle is placed in a light beam, the fissure may be

partially illuminated or it may be completely shadowed. In either instance, the surface comprised by the fissure walls will probably underregister on a light-transmission measurement. Estimating the size of such hidden areas can undoubtedly be improved by establishing the instrument's calibration on a carefully designed chemical or gas adsorption test instead of on a computation based on assumed particle shape.

The third topic pertains to modifying the instrument for flow-through measurements at a field site. For these measurements, the light emitter and light-detector must be mounted in a straight, open-ended conduit that completely blocks all sunlight and freely admits flowing water. Because the emitter and detector will probably be submerged for long periods of time, methods of automatically cleaning the optical surfaces must be developed.

In summary, the IR instrument shows considerable promise for measuring the surface area of particles in the size range from medium clay to very-fine sand. The IR apparatus has several advantages: It is simple to operate, it contains no moving parts, and it consumes little power. The last feature is particularly important at field sites where batteries are the only source of power.

REFERENCES

Orr, Clyde Jr., and DallaValle, J. M., 1959, Fine particle measurement, New York, N. Y., The Macmillan Company, 353 p.

Oster, G., 1948, The scattering of light and its applications to chemistry. Chemical Review 43, p. 319-365.

Sinclair, D., 1950, Optical properties of aerosols, Handbook on Aerosols, Chap. 7, U.S. Atomic Energy Comm., Washington, D.C., p. 81-96.

Szalona, Joseph J., 1984, Test of an infrared light-emitting turbidimeter, Report CC of A Study of methods used in measurement and analysis of sediment loads in streams: Minneapolis, Minn., Federal Interagency Sedimentation Project, 18 p.